Soil carbon accrual and biopore formation across a plant diversity gradient

Kyungmin Kim[1,2,3,4], Maik Geers-Lucas[5], G. Philip Robertson[3,4,6] and Alexandra Kravchenko[3,4]

[1]Department of Agricultural Biotechnology, Seoul National University, Seoul, Korea
[2]Institute of Plant Environmental Science, Research Institute of Agriculture and Life Sciences, Seoul National University, Seoul, Korea
[3]Department of Plant Soil and Microbial Sciences, Michigan State University, East Lansing, MI, USA
[4]DOE Great Lakes Bioenergy Research Center, Michigan State University, East Lansing, MI, USA
[5]Department of Soil Science, Technische Universität Berlin, Germany
[6]W.K. Kellogg Biological Station, Michigan State University, Hickory Corners, MI, USA

Correspondence to: Kyungmin Kim (km_kim@snu.ac.kr)

Abstract. Plant diversity promotes soil organic carbon (SOC) gains through intricate changes in root-soil interactions and their subsequent influence on soil physical and biological processes. We assessed SOC and pore characteristics of soils under a range of switchgrass-based plant systems 12 years after their establishment. The systems represented a gradient of plant diversity with species richness ranging from 1 to 30 species. We focused on soil biopores as indicators of the legacy of root activity and explored biopore relationships with SOC accumulation. Biopores were measured using X-ray computed micro-tomography.

Plant functional richness explained 29% of bioporosity and 36% of SOC variation, while bioporosity itself explained 36% of the variation in SOC. The most diverse plant system (30 species) had the highest SOC, while long-term bare soil fallow and monoculture switchgrass had the lowest. Of particular note was a two-species mixture of switchgrass (*Panicum virgatum* L.) and ryegrass (*Elymus canadensis*), which exhibited the highest bioporosity and achieved SOC levels comparable to those of the systems with 6 and 10 plant species, and were inferior only to the system with 30 species. We conclude that plant diversity may enhance SOC through biopore-mediated mechanisms and suggest a potential for identifying specific plant combinations that may be particularly efficient for fostering biopore formation and, subsequently, SOC sequestration.

1 Introduction

Plant diversity has been found to positively influence soil organic carbon (SOC) accumulation in various ecosystems, including grasslands (Lange et al., 2015; Sprunger and Robertson, 2018) and row crop agriculture (Liebman et al., 2013; McDaniel et al., 2014). Among the mechanisms through which higher plant diversity promotes SOC storage are i) high biomass and C inputs from roots (Yang and Tilman, 2020), ii) slower root decomposition in high diversity systems due to increased root C:N ratios (Chen et al., 2017), and iii) higher microbial activity enhanced by belowground inputs, where greater quantities of plant-added C are transformed into microbial biomass (Prommer et al., 2020; Lee et al., 2023) and then necromass (Qian et al., 2023; Mou et al., 2024). This microbially-processed C is then protected through physico-chemical associations with soil minerals (Cotrufo et al., 2022).

The quantity and chemical composition of C inputs from plant roots and soil biota play an important role in ensuring SOC gains (Berhongaray et al., 2019; Lehmann et al., 2020). For instance, extensive root growth and earthworm activity can facilitate the root exudates and earthworm secretions, which in turn stimulate microbial growth, C assimilation (Kuzyakov and Blagodatskaya, 2015), and the accumulation of microbial necromass (Banfield et al., 2018). Yet, the specific locations within the soil matrix where such inputs are added and their spatial distribution patterns can be an important driver in formation of SOC and its subsequent protection. In diverse plant communities, belowground competition among plants with contrasting root architectures can lead to greater root proliferation through the soil matrix, thereby increasing the density and spatial distribution of root channels that are in direct contact with the soil matrix (Gersani et al., 2001; Bargaz et al., 2017; Wang et al., 2017). Similarly, diverse plant communities exhibit increased activity of soil mesofauna such as earthworms, whereby earthworms create new biogenic channels that expand the contact surface between soil and organic inputs (Milcu et al., 2008; Kuzyakov and Kooch, 2024). The redistribution of these soil–organic matter interfaces varies considerably with plant diversity and species composition (Marshall et al., 2016; Zahorec et al., 2022). For instance, shifts in root morphology and spatial distribution in response to neighboring plant species (Bolte and Villanueva, 2006; Wang et al., 2014) indicate that the formation of root-derived channels and the localization of C storage depend on community composition. Likewise, findings that earthworm activity differs according to the presence of legumes (Eisenhauer et al., 2009) suggest that both the quantity and spatial pattern of SOC storage depend on plant species identity and diversity.

Analysis of root-soil and mesofauna-soil interactions in diverse perennial plant communities in situ is extremely challenging due to the opaque nature of soil and the difficulty of carrying out long-term (e.g., multiyear) continuous rhizobox or greenhouse studies. Thus, much knowledge is based on speculations from the data on root volumes and architecture generated upon disturbing the system to procure the roots and upon conducting the root measurements after cleaning away the soil (Lange et al., 2015). Likewise, earthworm–soil interactions have often been examined by simple comparisons between earthworm activity and soil carbon, while only a few studies have employed the technically demanding approach of artificially creating earthworm biopores with spatial information (Hoang et al., 2016). In contrast, sampling intact soil from long-term field studies and visualizing root residues, particulate organic matter (POM), and pores via X-ray computed micro-tomography (µCT) can generate helpful information on root-soil and earthworm-soil interactions (Helliwell et al., 2013). This is where identification and quantification of biopores can be particularly advantageous, because it allows capturing the legacy of root and mesofauna proliferation through the soil matrix and estimating the volume of the soil matrix that has received their C inputs in the past.

Biopores are the soil pores originated from biological activity such as plant root growth and the movement of earthworms and other soil fauna (Dexter, 1986; Blackwell et al., 1990). Biopores act as preferential pathways for root growth, organic matter inputs, water, and nutrient flow, thereby creating microenvironments that favor microbial colonization and necromass accumulation (Guhra et al., 2022; Kautz et al., 2015; Wendel et al., 2022). Root-originated biopores, formed either by growth of living roots or by decomposition of old roots, are particularly significant as they are 40 times more abundant, especially in subsoils, compared to earthworm biopores (Banfield et al., 2018). Root biopores are tubular, round-shaped channels with sizes ranging from a few micron to several centimeters (Kautz, 2015). Since root inputs are primarily introduced into the soil through the biopores, they have >2.5 times higher soil C contents compared to bulk soil (Banfield et al., 2017). Rapid microbial

78 decomposition of plant residues and accumulation of microbial residues observed in root biopores (Banfield et al.,
79 2018) suggest that root biopore characteristics may reflect the physical preferences and biochemical processes
80 involved in the transformation and accumulation of plant-derived C.

81   Reuse of existing biopores by newly grown roots is a commonly observed process in annual crops such
82 as wheat, fodder radish, and spring barley (White and Kirkegaard, 2010; Wahlström et al., 2021). Switchgrass, a
83 North American prairie grass, currently actively explored as a potential bioenergy feedstock (Larnaudie et al.,
84 2022; Zegada-Lizarazu et al., 2022), is known for its particularly active use of old root channels (i.e., biopore
85 reuse), especially when grown in monoculture (Lucas et al., 2023). Because of their continuous reuse,
86 accompanied by repeated influxes of new C and stimulated microbiota, biopores in perennial plant systems can
87 be viewed as hotspots of C processing and are both a product of historic root-soil interactions and a current arena
88 of such interactions. Taken together, these considerations suggest that the morphology and spatial pattern of root
89 biopores may serve as an informative indicator of root-derived SOC within the soil matrix.

90   We posit that biopore information derived from X-ray µCT is particularly informative for assessing root
91 impacts and root–soil interactions in perennial plant systems. In species-rich perennial communities, interspecific
92 interactions generate complex root architectures and heterogeneous rooting pathways, which in turn produce
93 spatially variable inputs of root-derived SOC (Zahorec et al., 2021). In this context, increased root-originated
94 biopores (e.g., the volume fraction and connectivity) can indicate diversified root growth paths and intensified
95 root–soil contact in perennial systems. Accordingly, we hypothesize that higher plant diversity promotes the
96 abundance and formation of root biopores and that this enhanced biopore development is associated with greater
97 gains in SOC. Specifically, our objectives are to examine (i) how a plant-diversity gradient shapes soil-pore
98 characteristics, with emphasis on biopores, and (ii) whether the (bio)pore abundance is associated with SOC levels
99 accrued over the preceding 12 years.

2 Materials and Methods

2.1 Experimental site and soil sampling

102   Soil samples were collected from the Cellulosic Biofuel Diversity Experiment site established in 2008
103 at Kellogg Biological Station (KBS, 42°23´47˝ N, 85°22´26˝ W), a part of the KBS Long-Term Ecological
104 Research (LTER) program (Robertson and Hamilton, 2015). The soil is fine-loamy, mixed, mesic, Typic
105 Hapludalf (Kalamazoo loam). The experiment consists of twelve plant systems representing a 12-point gradient
106 of plant diversity (CE1-CE12), six of which were used in this study. Specifically, we sampled a bare soil system,
107 which was kept free of vegetation since 2016 after 8 years of continuous corn (CE1), a monoculture switchgrass
108 (*Panicum virgatum*, L.; var. Southlow) system (CE7), a mixture of two grass species, namely, switchgrass and
109 Canadian rye (*Elymus canadensis*, L.) (CE8), a mixture of six native grasses (CE9), a mixture of six native grasses
110 and four forbs (CE10), and a mixture of six native grasses and 24 forbs (CE12). Plant species of each system are
111 listed in Supplementary Table S1. The experiment is in a randomized complete block design with four replicated
112 9.1 m x 27.4 m plots for each plant system (https://lter.kbs.msu.edu/research/long-term-experiments/cellulosic-
113 biofuels-experiment/).

114   For soil pore analysis, intact soil cores (5 cm diameter (Ø) and 5 cm height) were taken from the 7-12
115   cm depth interval in July 2019. This depth encompasses the zone of greatest fine-root abundance and turnover,
116   where root-derived C inputs and microbial activity are most pronounced (Halli et al., 2022; Roosendaal et al.,
117   2016). Loose soil adjacent to each core was also procured for measurements of other soil characteristics. Two soil
118   cores were collected from each plot, for a total of 48 soil cores (6 systems x 4 replicate plots x 2 cores per plot).
119   Aboveground biomass was measured each autumn (Oct–Nov) from 2010 to 2019 in all plots except CE1 (bare
120   soil) (Fig. S1a). For the present analysis, we used the 2018 and 2019 biomass datasets (Fig. S1b). Soil sampling
121   for this study occurred in July 2019; thus, the 2019 fall biomass provides the most temporally proximate estimate
122   of aboveground production for the soils analyzed, while the 2018 biomass offers the preceding-year context and
123   helps mitigate interannual variability. The entire aboveground biomass from each plot was harvested with a mini
124   combine, leaving 10-15 cm of stubble, and weighed and subsampled for moisture content determination. Due to
125   destructive and intensive sampling required for belowground biomass quantification, such measurements could
126   not be undertaken. Therefore, all plant biomass estimates in this study are explicitly based on aboveground
127   components only.
128

2.2 Soil characteristics measured using destructively sampled soil

130   Soil moisture at the time of core sampling was determined gravimetrically using a 20 g subsample of
131   loose soil immediately upon collection. The remaining loose soil samples were air-dried for 2 days and sieved to
132   < 2 mm for further analysis.
133   SOC and total soil N were measured by combustion analysis using an elemental CN analyzer (Costech
134   Analytical Technologies Inc., CA, USA). SOC mineralization was measured via 10 d incubation: 10 g of air-dried
135   soil were brought to 20% gravimetric moisture, placed in a beaker that was then placed in a 450 mL Mason jar
136   with ~5 mL of purified water on the bottom for maintaining high humidity within the jar. Mason jars were kept
137   in the dark at 20 °C for 10 days, and CO_2 concentration in the headspace was measured for each jar using Infrared
138   Photoacoustic Spectroscopy (INNOVA Air Tech Instruments, Denmark).

2.3 Soil core scanning and pore structure analysis

140   Soil cores were subjected to X-ray computed micro-tomography (North Star Imaging, X3000, Rogers,
141   USA) to visualize and quantify soil pore structure. X-ray µCT is particularly suitable for biopore investigation
142   (Wendel et al., 2022), enabling the examination of accumulated evidence of past root-soil interactions (Helliwell
143   et al., 2013). The scanning was conducted with a projection energy level of 75 KV and 450 µA, with 2880
144   projections per scan. 3D reconstruction of the images was computed using efX-CT software (North Star Imaging,
145   Rogers, USA) obtaining a final scanning resolution of 18.2 µm. Reconstructed images were processed using Fiji
146   software (Schindelin et al., 2012) and simpleITK package in Python (Beare et al., 2018). A series of image pre-
147   processing steps was conducted using Fiji and its Xlib plugin (Münch and Holzer, 2008). Specifically, images
148   were cropped into 1500 x 1500 pixels with a height of 2240 pixels to remove artifacts near core edges. Then, a
149   2D non-local filter (sigma=0.1) was applied to reduce noise.

150   For pore segmentation, threshold values were obtained from eight segmentation methods, i.e., Otsu,
151   Kitler, Huang, Triangle, ISO, Li, Renyi, and Moments. Outliers that exceeded >1 standard deviation of the mean
152   were removed. This approach enabled us to minimize the side effects of using one specific thresholding method
153   and ensured robustness of the segmentation (Schlüter et al., 2014). Hereafter, we refer to the >18.2 μm Ø pores
154   as visible pores, and their total volume as visible porosity. Pore size distributions of visible pores were determined
155   by the Local Thickness method embedded in Fiji, which is based on maximal inscribed spheres approach (Silin
156   and Patzek, 2006). For biopore identification, the images were subjected to Tubeness filtering in Fiji to detect
157   tubular type pores of different radius. Detailed procedures for biopore segmentation are publicly available
158   (https://github.com/Maik-Lu/Roots_and_Biopores) (Lucas et al., 2022). Total volumes of visible pores and
159   biopores were presented as visible porosity and bioporosity. Surface area of biopores was calculated by applying
160   assumption that the biopore shape is cylindrical in a given radius, and the mean distance of soil matrix to biopores
161   was calculated using the Euclidean Distance Transform (3D) function in Fiji (Lucas et al., 2025).
162

2.4 Plant diversity indicators

164   Two plant diversity indicators were used in this study: i) plant species richness, and ii) plant functional
165   richness (Díaz and Cabido, 2001). Plant species richness was represented by the number of plant species in each
166   treatment, i.e., 0, 1, 2, 6, 10, and 30 for CE1, CE7, CE8, CE9, CE10, and CE12, respectively. For plant functional
167   richness we adopted the ecological concept of plant functional types, used to simplify plant diversity and behavior
168   in ecological models (McMahon et al., 2011). Specifically, we followed the approach used in grassland studies
169   (Mangan et al., 2011; Spiesman et al., 2018; Tilman et al., 2006) by separating species based on different
170   photosynthetic pathways (C3 vs. C4), and leaf shape (broad-leaf vs. grasses) to form three functional groups,
171   namely, C3 grasses, C4 grasses, and forbs. Based on species characteristics (Table S1), plant functional richness
172   of each treatment was equal to 0, 1, 2, 2, 3, and 3 for CE1, CE7, CE8, CE9, CE10, and CE12, respectively.
173

## 2.5 Statistical analysis

175   The statistical model for SOC, total soil N, C:N ratio, 10-day mineralization, visible porosity, and
176   bioporosity data consisted of plant system as a fixed effect, and experimental blocks and blocks by systems
177   interaction as random effects (Milliken and Johnson, 2009). The latter term, in essence, represents experimental
178   plots and was used as an error term to test the plant system effect. The statistical model for the aboveground
179   biomass measured during two consecutive years further included year and its interaction with the plant system as
180   fixed factors. The statistical model for pore and biopore size distribution data included the pore size class and its
181   interaction with plant system as fixed effects, and soil core nested within the plant system and experimental plot
182   as the random effect. When the ANOVA was significant, all pairwise mean comparisons among plant systems
183   were conducted within each pore size class. Normality was checked by visual inspection of normal probability
184   plots, and when found violated, the data were subjected to either square root or lognormal transformation prior to
185   the analyses. The equal variance assumption was tested by Levene's test, and when found to be violated, the
186   unequal variance model was fitted using the approach suggested by Milliken and Johnson (2009).

To explore associations of soil characteristics with pore and biopore data, the porosity and bioporosity from two intact cores of each plot were averaged, followed by linear regression analysis. All statistical analyses were conducted using SAS 9.4 software, using PROC MIXED and PROC REG procedure. Results are reported as statistically significant at $p<0.05$ and as trends at $p<0.1$. P-values < 0.1, < 0.05, and < 0.01 are marked with *, **, and ***, respectively.

3 Results

3.1 Plant biomass and SOC characteristics of the studied plant systems

Total aboveground biomass (2018-2019) tended to be higher in the most diverse systems (CE10 and CE12) than in grass-only systems (CE8 and CE9), while the monoculture switchgrass (CE7) was intermediate (p < 0.10, Fig. S1b). Total aboveground biomass was weakly correlated with plant species richness (Fig. S2a) and not correlated with plant functional richness (Fig. S2b). Total aboveground biomass was not correlated with SOC contents (Fig. S2c). The plant systems with the highest diversity (CE12) had markedly higher SOC as compared to the rest of the systems (Fig. 1a). However, an increase in plant diversity from a two-species (CE8) to six-species (CE9) and then to a ten-species (CE10) system did not affect SOC (Fig. 1a). Soil C:N ratio was smallest in monoculture switchgrass (CE7), and greatest in high diversity systems (CE10 and CE12) (p< 0.01, Fig. S3). C mineralization was highest in CE12, followed by bare soil (CE1), and CE8 (Fig. 1c). C mineralization was lowest in CE7 and CE10.
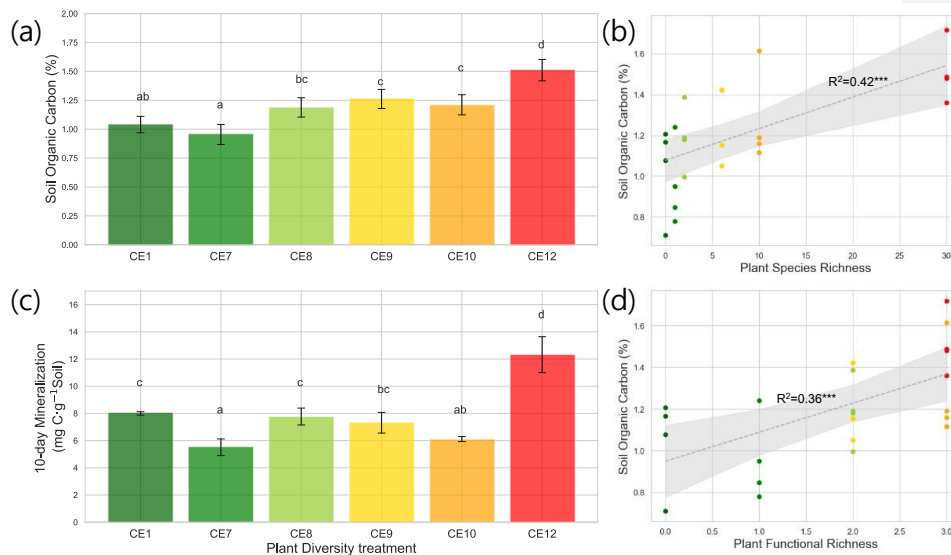
209 **Figure 1: Soil Organic Carbon (SOC) content (a) and 10-day mineralization (c) in the studied plant diversity systems**
210 **(CE1: Bare soil, CE7: Switchgrass, CE8: Switchgrass + Rye, CE9: 6 grasses, CE10: 6 grasses + 4 forbs. CE12: 6 grasses**
211 **+ 10 forbs). Correlations between SOC and Plant Species Richness (b), as well as Plant Functional Richness (d), are**
212 **shown. Letters indicate significant differences among plant diversity treatments (p< 0.05). Dotted gray lines in (b) and**
213 **(d) represent fitted regression models, with light gray shaded area denoting 95% confidence interval. R^2 values are**
214 **provided for each model. Asterisks (***) indicate statistically significant regression models at p< 0.01.**
215

216 **3.2 Biopore characteristics**

217   Plant systems affected pore size distributions (Fig. 2a), where CE8, CE10, and CE12 had the lowest
218 volumes of < 200 µm diameter pores and the highest volumes of >400 µm diameter pores, while an opposite trend
219 was observed for CE1, CE7, and CE9 systems. Biopores, which was segmented based on its tubular morphology,
220 tended to be larger than regular pores of arbitrary shapes (Fig. 2). For example, while the mode (i.e., the most
221 frequent value) pore diameter of the entire pore size distribution was ~100 µm (Fig. 2a), for biopores the modal
222 pore diamater was ~300 µm (Fig. 2b). Visible porosity (pores of > 18.2 µm diam.) was highest in CE9 followed
223 by CE8 (Fig. 3a). In contrast to visible porosity, bioporosity was the highest in CE8, which is comprised of
224 switchgrass and Canadian ryegrass (Fig. 3b). In addition to CE8, throughout the entire range of biopore sizes,
225 CE10 and CE12 also had consistently higher biopore volumes (Fig. 2b) as well as higher total bioporosity than
226 the rest of the systems (Fig. 3b). Total surface areas of biopores (all pores of < 1500 µm diam.) were highest in
227 CE7 and CE8, and lowest in CE1 (p< 0.05, Fig. 4a). Mean distance of soil matrix to biopores showed an opposite
228 trend from surface area, i.e., farthest in CE1 and CE9 and shortest in CE8 (p< 0.05, Fig. 4d).

7

(a)

(b)
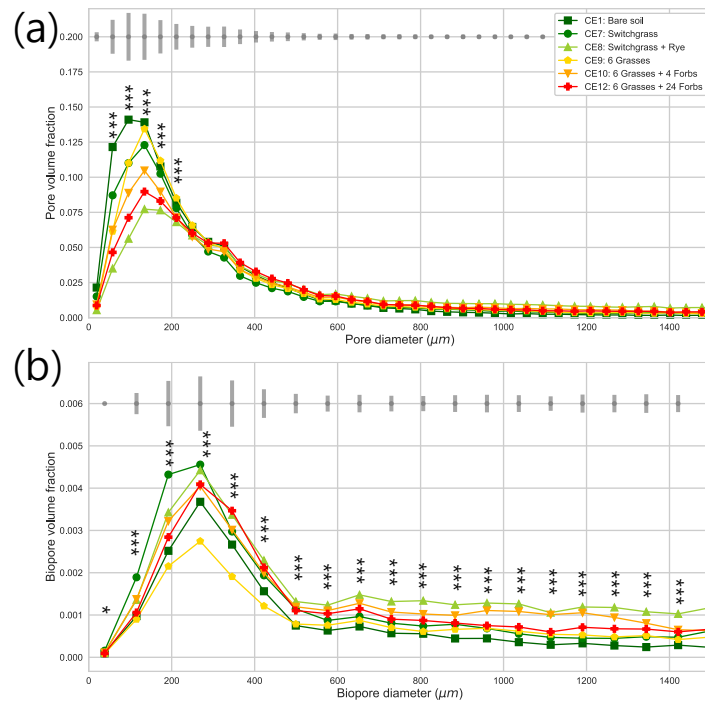
Figure 2: Pore size distribution (a) and biopore size distribution (b) in the studied plant diversity systems (CE1: Bare soil, CE7: Switchgrass, CE8: Switchgrass + Rye, CE9: 6 grasses, CE10: 6 grasses + 4 forbs. CE12: 6 grasses + 10 forbs). Gray bars indicate the least significant difference (LSD) in each (Bio)pore diameter group. Asterisks *** and * mark significant differences among the plant diversity treatments at each (Bio)pore diameter at p < 0.01 and p< 0.10 significance.

8

(a)

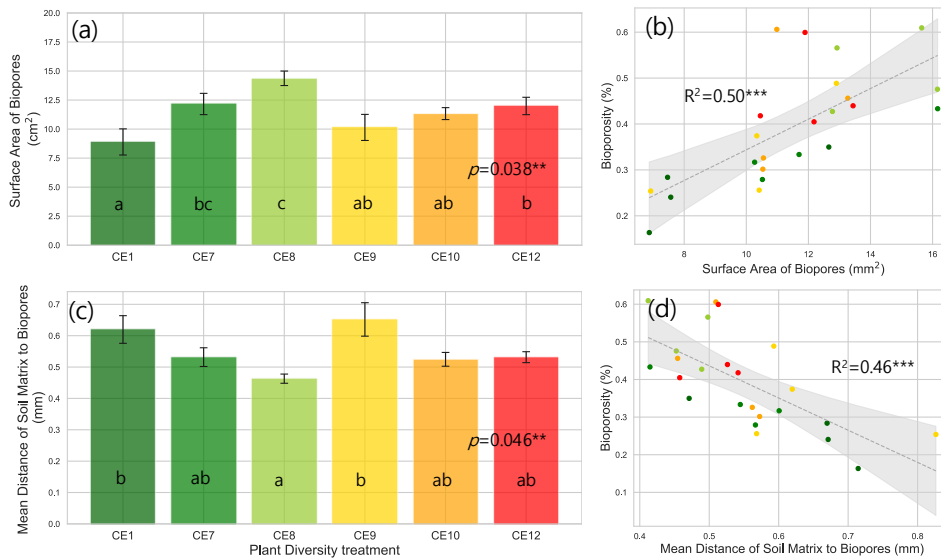(b)

236
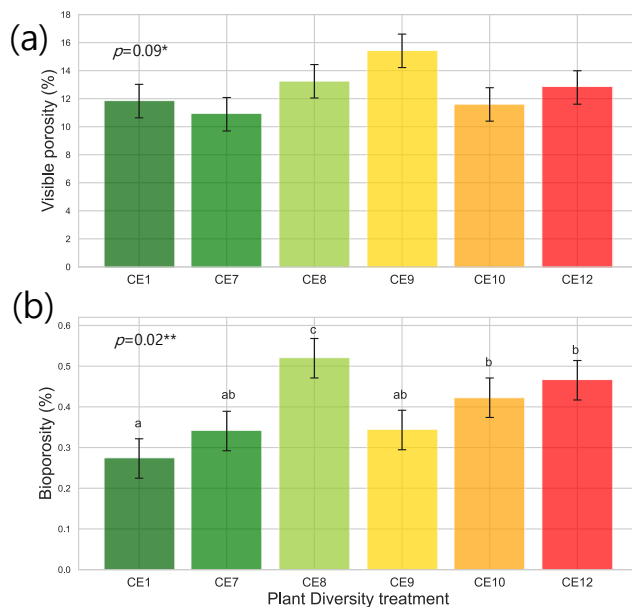
Figure 3: Visible porosity (a) and bioporosity (b) in the studied plant diversity systems (CE1: Bare soil, CE7:
238 **Switchgrass, CE8: Switchgrass + Rye, CE9: 6 grasses, CE10: 6 grasses + 4 forbs. CE12: 6 grasses + 10 forbs). Asterisks**
239 *** and ** indicate statistically significant differences among plant diversity treatments at p< 0.10 and 0.05, respectively.**
240 **Letters indicate significant differences among plant diversity treatments (p< 0.05).**

241 **3.3 Correlation between plant diversity, pore characteristics, and SOC**

242   Plant species richness and plant functional richness were both positively associated with SOC, with
243 species richness explaining 42% of the variance in SOC ($p < 0.01$; Fig. 1b) and functional richness explaining 36%
244 ($p < 0.01$; Fig. 1d). Within the pore metrics, biopore surface area was positively related to bioporosity ($R^2 = 0.50$,
245 $p < 0.01$; Fig. 4b), whereas the mean distance from the soil matrix to the nearest biopore was negatively related
246 to bioporosity ($R^2 = 0.46$, $p < 0.01$; Fig. 4d). Bioporosity increased with plant diversity. Species richness explained
247 10% of the variance in bioporosity ($p < 0.01$; Fig. S4a), and functional richness explained 29% ($p < 0.05$; Fig. 5a).
248 Consistent with these patterns, bioporosity was positively correlated with SOC ($R^2 = 0.36$, $p < 0.01$; Fig. 5b).
249

Figure 4: Surface area of biopores (a) and mean distance of soil matrix to biopores (c) in the studied plant diversity systems (CE1: Bare soil, CE7: Switchgrass, CE8: Switchgrass + Rye, CE9: 6 grasses, CE10: 6 grasses + 4 forbs. CE12: 6 grasses + 10 forbs). Correlations between bioporosity and surface area of biopores (b), as well as mean distance of soil matrix to biopores (d), are shown. Letters indicate significant differences among plant diversity treatments ($p < 0.05$). Dotted gray lines in (b) and (d) represent fitted regression models, with light gray shaded area denoting 95% confidence interval. R^2 values are provided for each model. Asterisks (***) indicate statistically significant regression models at $p < 0.01$.
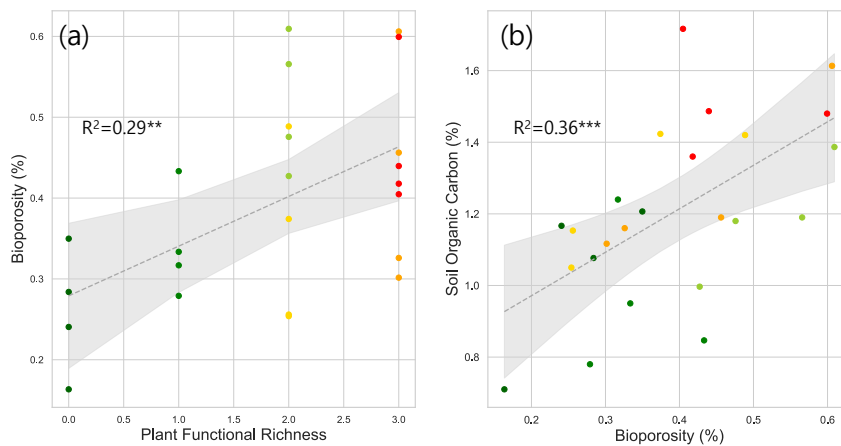
Figure 5: Correlation between plant functional richness and bioporosity (a), and between bioporosity and SOC (b). R^2 values are provided for each model. Dotted gray lines represent fitted regression models, with light gray shaded area

10

262   **denoting 95% confidence interval. Asterisks ** and *** indicate statistically significant regression models at p< 0.05**

263   **and 0.01, respectively.**

264   **4 Discussion**

265   **4.1 Biopores link plant diversity and SOC accumulation**

266   Consistent with our expectations and previous literature (Lange et al., 2015; Prommer et al., 2020; Yang

267   and Tilman, 2020), 12 years of contrasting vegetation was sufficient to develop differences in SOC among the

268   studied plant systems, with the highest SOC observed in the soil under the most diverse plant community (Fig. 1a,

269   b, and d). However, the lack of correlation between the plant aboveground biomass and SOC observed here (Fig.

270   S2c) suggests that greater plant biomass did not itself significantly contribute to SOC increases. This lack of

271   impact is even more obvious when comparing CE7 (monoculture) and CE8 (two-species system), where CE8 had

272   the lowest aboveground biomass but its SOC was comparable to that from the systems with 3~5 times higher plant

273   species richness and higher aboveground biomass (CE9 and 10, Fig. 1a and S1b).

274   The positive association between SOC and bioporosity was another result consistent with our

275   expectations (Fig. 5b). The correlation between plant richness and SOC was largely driven by the highest species

276   richness of 30, which was a high leverage point in our regression analysis (Fig. 1b and d). Thus, even though the

277   R^2 for bioporosity-SOC regression was lower than that from species richness-SOC (0.36 vs. 0.42), bioporosity

278   could be viewed as a better predictor of SOC. Moreover, the CE8 system with its unexpectedly high SOC turned

279   out to have higher bioporosity and higher volumes of biopores of all sizes than the other studied systems (Figs.

280   2b and 3b). This observation is consistent with previous reports identifying biopores as sites of high inputs of labile

281   substrates (Pierret et al., 1999; Xiong et al., 2022), increased microbial abundance and activity (Wendel et al.,

282   2022), and enhanced necromass accumulation (Banfield et al., 2018), all of which highlight the role of biopores

283   in contributing to SOC accrual. It should be noted that belowground biomass was not directly measured in this

284   study, which may have influenced estimates of biopore-related parameters. Direct belowground measurements

285   would allow disentangling root-biomass–driven biopore formation from species-interaction effects, and would

286   further clarify the contribution of belowground biomass to SOC accrual and the independent role of biopores.

287   The biopores in CE8 had the greatest surface area, followed by the most diverse system (Fig. 4a). The

288   mean distance of soil matrix to biopores was the shortest in CE8, followed by diverse systems (CE10 and CE12)

289   (Fig. 4c). The surface area of biopores is critical as it represents the specific portion of the soil matrix that directly

290   intercepts root-derived C inputs, i.e., rhizodeposits (Keller et al., 2021) and decomposed root residues processed

291   by soil microbes (Kim et al., 2022). A shorter mean distance from soil matrix to biopores indicates that root-

292   derived C was accessible to a large community of soil microorganisms, probably facilitating efficient transfer and

293   sequestration of microbially processed C into the soil matrix (Kravchenko et al., 2019). These findings emphasize

294   the currently underestimated importance of formation, abundance, and surface properties of biopores in affecting

295   soil biochemical status, specifically, influencing plant-derived inputs and their potential protection within the soil

296   matrix. Our study suggests that this role might be particularly pronounced in ecosystems with high plant species

297   diversity.

298   Our C mineralization results (Fig. 1c) did not much correspond with previous reports indicating that

299   higher plant diversity enhances microbial C use efficiency (Eisenhauer et al., 2009), likely driven by greater

11

300 chemical heterogeneity and enhanced substrate accessibility to soil microbes (Mellado-Vázquez et al., 2016;
301 Domeignoz-Horta et al., 2024). We suggest that future studies incorporate more detailed assessments of microbial
302 biomass, community composition, and diversity to better elucidate carbon processes occurring in biopores. These
303 inconsistencies highlight the need for further investigation of microbial activities and net C balance to identify the
304 specific microbial pathways operating in biopores. In particular, the integration of X-ray µCT with pore-scale
305 microbial analyses, as recently demonstrated by Li et al. (2024), represents a promising approach to advance our
306 understanding of SOC accumulation mediated by soil microorganisms in biopores structures.

307 **4.2 Future research directions: winning plant species combinations?**

308 Interestingly, while bioporosity was not affected by the number of plant species within the system, it
309 was positively correlated with the systems' functional diversity (Fig. 5a). This implies that greater diversity of
310 functional groups – rather than a greater diversity of plant species per se – may lead to a more thorough exploration
311 of the soil matrix in part through biopore formation, subsequently enhancing SOC accumulation. Moreover, our
312 results suggest that certain combinations of plant species, e.g., CE8 (Switchgrass + Canadian rye) in this study,
313 can be more "effective" in building biopores, and potentially furthering SOC accumulation through rapid
314 processing of added substrates (Banfield et al., 2017; Banfield et al., 2018). We hypothesize that Canadian rye
315 could be viewed as a species with a keystone effect on bioporosity and SOC accumulation.

316 A "keystone effect" refers to beneficial effect of a certain plant species on ecosystem function (Mills et
317 al., 1993). For instance, legume species added to grasslands have been found to disproportionately affect biomass
318 productivity and root C accrual (Minns et al., 2001; Fornara and Tilman, 2008; Lange et al., 2015; Yang et al.,
319 2019) due to N assimilation by legumes and consequent utilization of that N by grasses (Minns et al., 2001;
320 Mangan et al., 2011; Mou et al., 2024). Introduction of a C3 plant, i.e., Canadian rye, into a monoculture C4
321 switchgrass community may have altered switchgrass root growth and exudation patterns. This conjecture is
322 supported by a report on sensitivity of chemical composition of switchgrass root exudates to neighbouring plant
323 species (e.g., C3 *Koeleria macrantha* Ledeb.), with subsequent increases in microbial biomass C and changes in
324 bacterial diversity in the switchgrass rhizosphere (Ulbrich et al., 2022). We see the need for further investigation
325 into the role that individual members of grassland communities may play in stimulating soil pore structure
326 development and SOC accumulation. Identifying keystone species enabling more efficient C accumulation can
327 guide plant restoration and SOC accrual efforts.

328 **5. Conclusion**

329 The 12-year grassland experiment demonstrates that SOC accumulation is governed by plant diversity, with the
330 benefits of high plant diversity being, in part, exhibited via development of biopores. Yet, certain species
331 combinations may lead to biopore formation and SOC accumulation benefits disproportional to the actual level
332 of the plant system diversity. Specifically, the two-species mixture of C4 switchgrass and C3 Canadian rye created
333 the greatest bioporosity, shortest mean soil-to-pore distance, and the largest biopore surface area, thereby
334 accelerating microbial processing and stabilization of root-derived C in the surrounding matrix. These findings
335 highlight bioporosity as a more reliable proxy for SOC gains than plant species number alone, and point to
336 potential existence of specific "keystone" species combinations that may disproportionately enhance soil structure

337 and C sequestration. Identifying and deploying such functionally complementary plant species can offer a targeted
338 pathway for optimizing grassland restoration and long-term SOC storage.

346 **Code/Data availability**

347 ~~The datasets generated during and/or analyzed during the current study are available upon request.~~
348 All data underlying the main article are provided in the Supplementary Information (Tables S2 and S3).

349 **Author contribution**

350 K. K Formal analysis, investigation, Writing-original draft, visualization
351 M.G: Software, Validation, Writing-Review & Editing
352 G. P. R: Resources, Project administration, Writing-Review & Editing
353 A. K: Conceptualization, Resources, Writing-Review & Editing, Supervision, Funding acquisition

354 **Competing interests**

355 The authors declare that they have no known competing financial interests or personal relationships that could
356 have appeared to influence the work reported in this paper.

357 **References**

358 Banfield, C.C., Dippold, M.A., Pausch, J., Hoang, D.T., Kuzyakov, Y., 2017. Biopore history determines the
359 microbial community composition in subsoil hotspots. Biology and Fertility of Soils 53, 573-588.
360 Banfield, C.C., Pausch, J., Kuzyakov, Y., Dippold, M.A., 2018. Microbial processing of plant residues in the
361 subsoil–The role of biopores. Soil Biology and Biochemistry 125, 309-318.
362 Bargaz, A., Noyce, G.L., Fulthorpe, R., Carlsson, G., Furze, J.R., Jensen, E.S., Dhiba, D., Isaac, M.E., 2017.
363 Species interactions enhance root allocation, microbial diversity and P acquisition in intercropped wheat and
364 soybean under P deficiency. Applied Soil Ecology 120, 179-188.
365 Beare, R., Lowekamp, B., Yaniv, Z., 2018. Image segmentation, registration and characterization in R with
366 SimpleITK. Journal of statistical software 86.
367 Berhongaray, G., Cotrufo, F.M., Janssens, I.A., Ceulemans, R., 2019. Below-ground carbon inputs contribute
368 more than above-ground inputs to soil carbon accrual in a bioenergy poplar plantation. Plant and soil 434, 363-
369 378.
370 Blackwell, P., Green, T., Mason, W., 1990. Responses of biopore channels from roots to compression by vertical
371 stresses. Soil Science Society of America Journal 54, 1088-1091.

Bolte, A., Villanueva, I., 2006. Interspecific competition impacts on the morphology and distribution of fine roots in European beech (Fagus sylvatica L.) and Norway spruce (Picea abies (L.) Karst.). European Journal of Forest Research 125, 15-26.

Chen, H., Mommer, L., Van Ruijven, J., De Kroon, H., Fischer, C., Gessler, A., Hildebrandt, A., Scherer-Lorenzen, M., Wirth, C., Weigelt, A., 2017. Plant species richness negatively affects root decomposition in grasslands. Journal of Ecology 105, 209-218.

Cotrufo, M.F., Haddix, M.L., Kroeger, M.E., Stewart, C.E., 2022. The role of plant input physical-chemical properties, and microbial and soil chemical diversity on the formation of particulate and mineral-associated organic matter. Soil Biology and Biochemistry 168, 108648.

Dexter, A., 1986. Model experiments on the behaviour of roots at the interface between a tilled seed-bed and a compacted sub-soil: III. Entry of pea and wheat roots into cylindrical biopores. Plant and soil 95, 149-161.

Díaz, S., Cabido, M., 2001. Vive la différence: plant functional diversity matters to ecosystem processes. Trends in ecology & evolution 16, 646-655.

Domeignoz-Horta, L.A., Cappelli, S.L., Shrestha, R., Gerin, S., Lohila, A.K., Heinonsalo, J., Nelson, D.B., Kahmen, A., Duan, P., Sebag, D., 2024. Plant diversity drives positive microbial associations in the rhizosphere enhancing carbon use efficiency in agricultural soils. Nature communications 15, 8065.

Eisenhauer, N., Lanoue, A., Strecker, T., Scheu, S., Steinauer, K., Thakur, M. P., & Mommer, L., 2017. Root biomass and exudates link plant diversity with soil bacterial and fungal biomass. *Scientific reports*, *7*(1), 1-8.

Fornara, D., Tilman, D., 2008. Plant functional composition influences rates of soil carbon and nitrogen accumulation. Journal of Ecology 96, 314-322.

Eisenhauer, N., Milcu, A., Sabais, A.C., Bessler, H., Weigelt, A., Engels, C., Scheu, S., 2009. Plant community impacts on the structure of earthworm communities depend on season and change with time. Soil Biology and Biochemistry 41, 2430-2443.

Gersani, M., Brown, J.S., O'Brien, E.E., Maina, G.M., Abramsky, Z., 2001. Tragedy of the commons as a result of root competition. Journal of Ecology 89, 660-669.

Guhra, T., Stolze, K., Totsche, K.U., 2022. Pathways of biogenically excreted organic matter into soil aggregates. Soil Biology and Biochemistry 164, 108483.

Halli, H. M., Govindasamy, P., Choudhary, M., Srinivasan, R., Prasad, M., Wasnik, V. K., Yadav, V., Singh, A.K., Kumar, S. , Vijay, D., and Pathak, H. (2022). Range grasses to improve soil properties, carbon sustainability, and fodder security in degraded lands of semi-arid regions. *Science of the Total Environment*, *851*, 158211.

Helliwell, J.R., Sturrock, C.J., Grayling, K.M., Tracy, S.R., Flavel, R., Young, I., Whalley, W., Mooney, S.J., 2013. Applications of X-ray computed tomography for examining biophysical interactions and structural development in soil systems: a review. European Journal of Soil Science 64, 279-297.

Hoang, D.T., Pausch, J., Razavi, B.S., Kuzyakova, I., Banfield, C.C., Kuzyakov, Y., 2016. Hotspots of microbial activity induced by earthworm burrows, old root channels, and their combination in subsoil. Biology and Fertility of Soils 52, 1105-1119.

Kautz, T., 2015. Research on subsoil biopores and their functions in organically managed soils: A review. Renewable Agriculture and Food Systems 30, 318-327.

Keller, A.B., Brzostek, E.R., Craig, M.E., Fisher, J.B., Phillips, R.P., 2021. Root-derived inputs are major contributors to soil carbon in temperate forests, but vary by mycorrhizal type. Ecology letters 24, 626-635.

Kim, K., Gil, J., Ostrom, N.E., Gandhi, H., Oerther, M.S., Kuzyakov, Y., Guber, A.K., Kravchenko, A.N., 2022. Soil pore architecture and rhizosphere legacy define N2O production in root detritusphere. Soil Biology and Biochemistry 166, 108565.

Kravchenko, A., Guber, A., Razavi, B., Koestel, J., Quigley, M., Robertson, G., Kuzyakov, Y., 2019. Microbial spatial footprint as a driver of soil carbon stabilization, Nat. Commun., 10, 3121.

Kravchenko, A.N., Zheng, H., Kuzyakov, Y., Robertson, G.P., Guber, A.K., 2021. Belowground interplant carbon transfer promotes soil carbon gains in diverse plant communities. Soil Biology & Biochemistry 159.

Kuzyakov, Y., Blagodatskaya, E., 2015. Microbial hotspots and hot moments in soil: concept & review. Soil Biology and Biochemistry 83, 184-199.

Kuzyakov, Y., Kooch, Y., 2024. Earthworm Biopores for Transport and Nutrient Cycling, Earthworms and Ecological Processes. Springer, pp. 417-432.

Lange, M., Eisenhauer, N., Sierra, C.A., Bessler, H., Engels, C., Griffiths, R.I., Mellado-Vázquez, P.G., Malik, A.A., Roy, J., Scheu, S., 2015. Plant diversity increases soil microbial activity and soil carbon storage. Nature communications 6, 6707.

Larnaudie, V., Ferrari, M.D., Lareo, C., 2022. Switchgrass as an alternative biomass for ethanol production in a biorefinery: Perspectives on technology, economics and environmental sustainability. Renewable and Sustainable Energy Reviews 158, 112115.

Lee, J.H., Lucas, M., Guber, A.K., Li, X., Kravchenko, A.N., 2023. Interactions among soil texture, pore structure, and labile carbon influence soil carbon gains. Geoderma 439, 116675.

14

431 Lee, J.H., Ulbrich, T.C., Oerther, M., Kuzyakov, Y., Guber, A.K., Kravchenko, A.N., 2025. Belowground plant
432 carbon and nitrogen exchange: plant-derived carbon inputs and pore structure formation. Soil Biology and
433 Biochemistry 207, 109833.
434 Li, Z., Kravchenko, A.N., Cupples, A., Guber, A.K., Kuzyakov, Y., Philip Robertson, G., Blagodatskaya, E., 2024.
435 Composition and metabolism of microbial communities in soil pores. Nature communications 15, 3578.
436 Lehmann, J., Hansel, C.M., Kaiser, C., Kleber, M., Maher, K., Manzoni, S., Nunan, N., Reichstein, M., Schimel,
437 J.P., Torn, M.S., 2020. Persistence of soil organic carbon caused by functional complexity. Nature Geoscience 13,
438 529-534.
439 Liebman, M., Helmers, M.J., Schulte, L.A., Chase, C.A., 2013. Using biodiversity to link agricultural productivity
440 with environmental quality: Results from three field experiments in Iowa. Renewable Agriculture and Food
441 Systems 28, 115-128.
442 Lucas, M., Nguyen, L.T., Guber, A., Kravchenko, A.N., 2022. Cover crop influence on pore size distribution and
443 biopore dynamics: Enumerating root and soil faunal effects. Frontiers in Plant Science 13, 928569.
444 Lucas, M., Santiago, J.P., Chen, J., Guber, A., Kravchenko, A., 2023. The soil pore structure encountered by roots
445 affects plant-derived carbon inputs and fate. New Phytologist 240, 515-528.
446 Mangan, M.E., Sheaffer, C., Wyse, D.L., Ehlke, N.J., Reich, P.B., 2011. Native perennial grassland species for
447 bioenergy: establishment and biomass productivity. Agronomy Journal 103, 509-519.
448 Lucas, M., Gil, J., Robertson, G., Ostrom, N., Kravchenko, A., 2025. Changes in soil pore structure generated by
449 the root systems of maize, sorghum and switchgrass affect in situ N2O emissions and bacterial denitrification.
450 Biology and Fertility of Soils 61, 367-383.
451 Marshall, A.H., Collins, R.P., Humphreys, M.W., Scullion, J., 2016. A new emphasis on root traits for perennial
452 grass and legume varieties with environmental and ecological benefits. Food and energy security 5, 26-39.
453 McDaniel, M.D., Tiemann, L.K., Grandy, A.S., 2014. Does agricultural crop diversity enhance soil microbial
454 biomass and organic matter dynamics? A meta-analysis. Ecological Applications 24, 560-570.
455 McMahon, S.M., Harrison, S.P., Armbruster, W.S., Bartlein, P.J., Beale, C.M., Edwards, M.E., Kattge, J.,
456 Midgley, G., Morin, X., Prentice, I.C., 2011. Improving assessment and modelling of climate change impacts on
457 global terrestrial biodiversity. Trends in ecology & evolution 26, 249-259.
458 Mellado-Vázquez, P.G., Lange, M., Bachmann, D., Gockele, A., Karlowsky, S., Milcu, A., Piel, C., Roscher, C.,
459 Roy, J., Gleixner, G., 2016. Plant diversity generates enhanced soil microbial access to recently photosynthesized
460 carbon in the rhizosphere. Soil Biology and Biochemistry 94, 122-132.
461 Milcu, A., Partsch, S., Scherber, C., Weisser, W. W., & Scheu, S., 2008. Earthworms and legumes control litter
462 decomposition in a plant diversity gradient. *Ecology*, *89*(7), 1872-1882.
463 Milliken, G.A., Johnson, D.E., 2009. Analysis of Messy Data Volume 1. (No Title).
464 Mills, L.S., Soulé, M.E., Doak, D.F., 1993. The keystone-species concept in ecology and conservation. BioScience
465 43, 219-224.
466 Minns, A., Finn, J., Hector, A., Caldeira, M., Joshi, J., Palmborg, C., Schmid, B., Scherer-Lorenzen, M., Spehn,
467 E., Troumbis, A., project, t.B., 2001. The functioning of European grassland ecosystems: potential benefits of
468 biodiversity to agriculture. Outlook on AGRICULTURE 30, 179-185.
469 Mou, X., Lv, P., Jia, B., Mao, H., Zhao, X., 2024. Plant species richness and legume presence increase microbial
470 necromass carbon accumulation. Agriculture, Ecosystems & Environment 374, 109196.
471 Mueller, C.W., Baumert, V., Carminati, A., Germon, A., Holz, M., Kögel-Knabner, I., Peth, S., Schlüter, S., Uteau,
472 D., Vetterlein, D., 2024. From rhizosphere to detritusphere–Soil structure formation driven by plant roots and the
473 interactions with soil biota. Soil Biology and Biochemistry 193, 109396.
474 Münch, B., Holzer, L., 2008. Contradicting geometrical concepts in pore size analysis attained with electron
475 microscopy and mercury intrusion. Journal of the American Ceramic Society 91, 4059-4067.
476 Newman, E.I., Ritz, K., 1986. Evidence of the pathways of phosphorus transfer between vesicular-arbuscular
477 mycorrhizal plants. New Phytologist 104, 77-87.
478 Pierret, A., Moran, C., Pankhurst, C., 1999. Differentiation of soil properties related to the spatial association of
479 wheat roots and soil macropores. Plant and soil 211, 51-58.
480 Prommer, J., Walker, T.W., Wanek, W., Braun, J., Zezula, D., Hu, Y., Hofhansl, F., Richter, A., 2020. Increased
481 microbial growth, biomass, and turnover drive soil organic carbon accumulation at higher plant diversity. Global
482 Change Biology 26, 669-681.
483 Qian, Z., Li, Y., Du, H., Wang, K., Li, D., 2023. Increasing plant species diversity enhances microbial necromass
484 carbon content but does not alter its contribution to soil organic carbon pool in a subtropical forest. Soil Biology
485 and Biochemistry 187, 109183.
486 Quigley, M., Kravchenko, A., 2022. Inputs of root-derived carbon into soil and its losses are associated with pore-
487 size distributions. Geoderma 410, 115667.
488 Robertson, G.P., Hamilton, S.K., 2015. Long-term ecological research at the Kellogg Biological Station LTER
489 site. The ecology of agricultural landscapes: Long-term research on the path to sustainability 1, 32.

15

Roosendaal, D., Stewart, C.E., Denef, K., Follett, R.F., Pruessner, E., Comas, L.H., Varvel, G.E., Saathoff, A., Palmer, N., Sarath, G., 2016. Switchgrass ecotypes alter microbial contribution to deep-soil C. Soil 2, 185-197.

Schindelin, J., Arganda-Carreras, I., Frise, E., Kaynig, V., Longair, M., Pietzsch, T., Preibisch, S., Rueden, C., Saalfeld, S., Schmid, B., 2012. Fiji: an open-source platform for biological-image analysis. Nature methods 9, 676-682.

Schlüter, S., Sheppard, A., Brown, K., Wildenschild, D., 2014. Image processing of multiphase images obtained via X-ray microtomography: A review. Water Resources Research 50, 3615-3639.

Silin, D., Patzek, T., 2006. Pore space morphology analysis using maximal inscribed spheres. Physica A: Statistical mechanics and its applications 371, 336-360.

Spiesman, B.J., Kummel, H., Jackson, R.D., 2018. Carbon storage potential increases with increasing ratio of C 4 to C 3 grass cover and soil productivity in restored tallgrass prairies. Oecologia 186, 565-576.

Sprunger, C.D., Robertson, G.P., 2018. Early accumulation of active fraction soil carbon in newly established cellulosic biofuel systems. Geoderma 318, 42-51.

Tilman, D., Reich, P. B., & Knops, J. M. 2006. Biodiversity and ecosystem stability in a decade-long grassland experiment. *Nature*, *441*(7093), 629-632.

Ulbrich, T.C., Rivas-Ubach, A., Tiemann, L.K., Friesen, M.L., Evans, S.E., 2022. Plant root exudates and rhizosphere bacterial communities shift with neighbor context. Soil Biology and Biochemistry 172, 108753.

Wahlström, E.M., Kristensen, H.L., Thomsen, I.K., Labouriau, R., Pulido-Moncada, M., Nielsen, J.A., Munkholm, L.J., 2021. Subsoil compaction effect on spatio-temporal root growth, reuse of biopores and crop yield of spring barley. European Journal of Agronomy 123, 126225.

Wang, B., Zhang, W., Ahanbieke, P., Gan, Y., Xu, W., Li, L., Christie, P., Li, L., 2014. Interspecific interactions alter root length density, root diameter and specific root length in jujube/wheat agroforestry systems. Agroforestry systems 88, 835-850.

Wang, X.-Y., Ge, Y., Wang, J., 2017. Positive effects of plant diversity on soil microbial biomass and activity are associated with more root biomass production. Journal of Plant Interactions 12, 533-541.

Wendel, A.S., Bauke, S.L., Amelung, W., Knief, C., 2022. Root-rhizosphere-soil interactions in biopores. Plant and soil 475, 253-277.

White, R.G., Kirkegaard, J.A., 2010. The distribution and abundance of wheat roots in a dense, structured subsoil– implications for water uptake. Plant, cell & environment 33, 133-148.

Xiong, P., Zhang, Z., Peng, X., 2022. Root and root-derived biopore interactions in soils: A review. Journal of Plant Nutrition and Soil Science 185, 643-655.

Yang, Y., Tilman, D., 2020. Soil and root carbon storage is key to climate benefits of bioenergy crops. Biofuel Research Journal 7, 1143-1148.

Yang, Y., Tilman, D., Furey, G., Lehman, C., 2019. Soil carbon sequestration accelerated by restoration of grassland biodiversity. Nature communications 10, 718.

Zahorec, A., Reid, M.L., Tiemann, L.K., Landis, D.A., 2022. Perennial grass bioenergy cropping systems: Impacts on soil fauna and implications for soil carbon accrual. GCB Bioenergy 14, 4-23.

Zegada-Lizarazu, W., Zanetti, F., Di Virgilio, N., Monti, A., 2022. Is switchgrass good for carbon savings? Long-term results in marginal land. GCB Bioenergy 14, 814-823.